J Eng Math (2007) 57:1–21
DOI 10.1007/s10665-006-9048-z

ORIGINAL PAPER

Parametric resonance in an oscillating water column

Arturo Olvera · Esteban Prado · Steven Czitrom

Received: 14 December 2004 / Accepted: 23 March 2006 / Published online: 22 August 2006

Abstract A common type of device for wave-energy extraction is an oscillating water column (OWC) with a compression chamber. Peak performance of most OWC systems occurs at resonance with the driving waves. At resonance, oscillations increase linearly in time until damping inhibits further growth. Parametric resonance is introduced as a means of exciting the oscillations of the water column. In parametric resonance, oscillations increase exponentially in time. The use of this kind of resonance may increase the performance of OWC systems. This type of resonance occurs when one of the parameters in an oscillator varies periodically. Asymptotic methods are used to study the nonlinear dynamics of an OWC with parametric resonance. These results are compared with those of a numerical model of a real experimental laboratory setup.

Keywords Multiple-scale method · Nonlinear oscillations · Oscillating water column · Parametric resonance

1 Introduction

Harnessing the energy of ocean waves has long sparked the imagination of those witnessing the endless battering of waves on beaches and coasts. In the past decades, significant advances to convert this energy to electric power have been made possible thanks to the advent of sophisticated computing and hardware technologies, although widespread economically competitive and storm-proof devices remain mostly elusive. Highly ingenious devices have been proposed by Salter [1], McCormick [2], the Kvaerner OWC [3], etc. Since 2003, the Dragon, a floating device which amplifies waves and spills run-up water into a reservoir which feeds conventional turbines, has been producing electric power successfully and feeding the Danish grid on a commercial basis [4]. Pelamis, a promising device which

A. Olvera (✉)
FENOMEC and IIMAS, UNAM, México, D.F., México
e-mail: aoc@mym.iimas.unam.mx

E. Prado · S. Czitrom
ICMyL, UNAM, México, D.F., México

comprises a series of semi-submerged articulated cylinders with power hydraulic compressors at the joints is at the prototype level [5]. Submerged buoys which drive the stators of linear electrical generators are also being tested [6]. Although there is much potential in waves as an alternative energy source, serious setbacks to the necessary research have been experienced in the past when some of these devices were destroyed by storms. Much research is now being directed to build storm-resistant devices.

One class of devices which have received much attention are based on a wave-driven oscillating water column (OWC) which compresses air in a chamber and forces it through a turbine to produce electricity. The development of these devices dates from the 1950s when Masuda [7] powered navigation signaling buoys with OWC-driven turbines. Falnes [8, pp. 225–259] pioneered theoretical studies of OWCs and showed that they are in effect mechanic oscillators forced by the wave-pressure signal. At present, various OWC-driven power-generating prototypes are being tested at Pico Island [9, 10] and on the northern Irish coast [11].

OWC-driven devices operate optimally at resonance when their natural frequency of oscillation coincides with that of the most energetic waves. Phase-locking mechanisms have been developed to increase their performance by taking advantage of wave energy, even when the devices are out of resonance [3]. Alternatively, dynamic tuning devices, based on a variable volume-air compression chamber, have been developed to maintain a resonant condition despite variations in the wave spectra to the most energetic waves [12].

Efficiency in wave-energy devices can also be substantially increased if the useful end-product energy is of an equivalent type (kinetic–kinetic). As an alternative application to electric generation, an oscillating water-column wave-driven seawater pump, which has potential for various coastal management purposes, such as the cleaning of contaminated areas and aquaculture, has been under development since the 1990s at the National University of Mexico [12]. A schematic diagram of the seawater pump can be seen in Fig. 1. The wave-induced pressure signal at the mouth of the resonant duct drives an oscillating flow that spills water into the compression chamber, and through the exhaust duct to the receiving body of water, with each passing wave. Air in the chamber behaves like a spring against which water in the resonant and exhaust ducts oscillates. Maximum efficiency at resonance can be maintained for different wave frequencies by means of a variable-volume compression chamber that adjusts the hardness of the air spring. In this paper, we explore alternatives to diversify the uses and the efficiency of such OWC seawater pumps.

In an oscillator, the normal modes of oscillation are a function of several parameters, such as the mass and the spring constant. When one of these parameters changes periodically, a small perturbation, under certain circumstances, can grow exponentially in time. This phenomenon is known as ‘parametric resonance’ [13, pp. 80–84]. In classical mechanics, it is known that, when this type of resonance occurs, energy

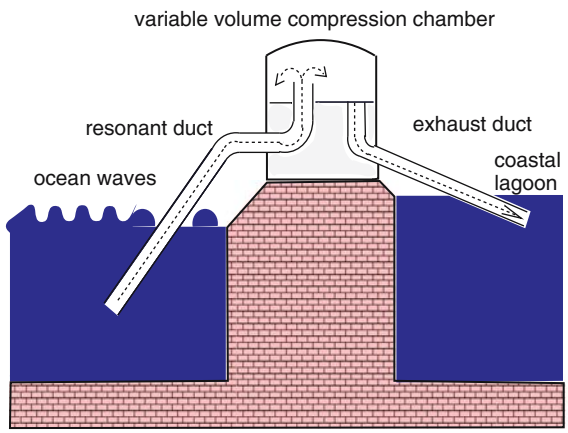

Fig. 1 Schematic diagram of the wave drive resonant seawater pump

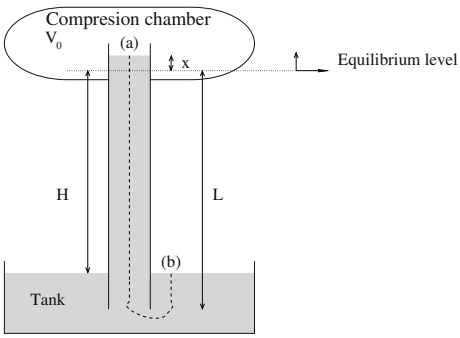

Fig. 2 Diagram of an oscillating water column with compression chamber

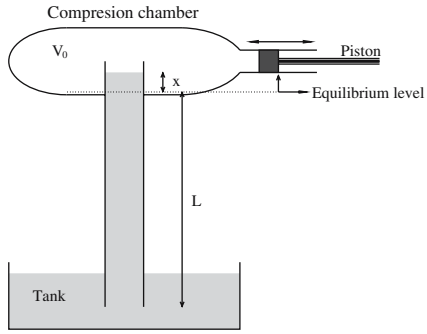

Fig. 3 Parametric excitation of an OWC. The compression chamber is perturbed by the action of the piston

is transferred with much greater efficiency than in ordinary resonance. A simple example of parametric resonance is the increased oscillations in a child's swing, in the absence of external forces. In this case, the parameter being rhythmically changed is the length of the rope, as the child rises and lowers his center of mass. The work exerted by the child in doing so is transformed very efficiently into mechanical oscillations. In this paper, some basic concepts of parametric resonance are explored as a possible way of improving the performance of OWC systems.

2 Mathematical model of an OWC

A simple model of a single oscillating water column (OWC) with a compression chamber is shown in Fig. 2. Assuming an ideal fluid, the dynamics of the water column can be compared to a mechanical spring, where the mass of the spring is the mass of water in the vertical column of length $L + x$. The restitutive forces of the spring model are given by the gravitational force and the difference of pressure exerted by the compression chamber. The total force is then conservative and it must be the gradient of some potential energy $\mathcal{V}(x)$. The kinetic energy is given by the product of the mass of the water column $(L + x)\rho\mathcal{A}_c$ and $\dot{x}^2/2$, where $\mathcal{A}_c$ is the area of the column, ρ is the fluid density and $\dot{x}$ is the velocity of the mass of water. This velocity is the change in time of the water top level in the column. Therefore, the kinetic energy can be computed as:

$$\mathcal{T} = \mathcal{A}_c\rho(L + x)\frac{\dot{x}^2}{2}. \tag{1}$$

The two restitutive forces, gravity and pressure in the compression chamber, maintain the water column at level H with respect to the water level in the tank. The first force is $F_g = -\rho\mathcal{A}_c x g$, where g is the gravitational acceleration and $\rho\mathcal{A}_c x$ is the mass of water above (or below) the equilibrium level. If we assume that heat exchange with the exterior is negligible, the adiabatic relation between pressure and volume is given by $PV^\gamma = P_0V_0^\gamma$, where P_0 and V_0 are the pressure and volume at the equilibrium level ($x = 0$) and γ is the adiabatic constant. The restitutive force is proportional to the difference of pressure $P - P_0$, substituting P from the adiabatic relation and taking the volume as $V = V_0 - \mathcal{A}_c x$, the restitutive force due to the compression chamber, is then:

$$F_{\text{ad}} = -(P - P_0)\mathcal{A}_c = -P_0\left(\left(1 - \frac{\mathcal{A}_c x}{V_0}\right)^{-\gamma} - 1\right)\mathcal{A}_c. \tag{2}$$

The pressure at equilibrium level is the difference between the atmospheric pressure (P_A) and the pressure required to lift the water column to an altitude H with respect to the water level in the tank, $P_0 = P_A - \rho g H$.

The Lagrangian function of our mechanical problem is:

$$\mathcal{L} = \mathcal{T} - \mathcal{V}, \tag{3}$$

where $-\partial\mathcal{V}/\partial x = F_{\text{ad}} + F_g$.

Using the Euler–Lagrange equation, $\frac{\mathrm{d}}{\mathrm{d}t}(\partial\mathcal{L}/\partial\dot{x}) - \partial\mathcal{L}/\partial x = 0$, we obtain the equation of motion of the oscillating water column:

$$(x + L(1+\eta))\ddot{x} + \frac{\dot{x}^2}{2} + gx + \frac{P_{\text{A}} - \rho g H}{\rho}\left(\left(1 - \frac{\mathcal{A}_{\text{c}} x}{V_0}\right)^{-\gamma} - 1\right) = 0, \tag{4}$$

where the parameter η is a fractional added length due to edge effects at the duct mouth [14, 15].

An alternative approach to obtain Eq. (4) is to consider a streamline which connects the free water surface (b) and the top of the water column (a) [16]. Applying the Bernoulli equation to the streamline from the point (a) to point (b), we can derive Eq. (4).

The OWC model was designed assuming an ideal fluid. For real fluids, Knott and Flower and Czitrom have successfully included viscous losses in this model [12, 16]. Nonlinear losses due to friction, vortex formation and radiation damping can be included in our model in the same way using:

$$\left(\frac{K}{2} + \frac{L}{D}f\right)\dot{x}|\dot{x}|, \tag{5}$$

where K is the vortex-formation energy-loss coefficient, D is the resonant duct diameter, f is the oscillating-flow friction coefficient.

In a recent publication [15] the sources of dissipation in gravity oscillations of a liquid column are described and an equation for the energy loss is derived. From their experiments they found that the change of the total energy ($\mathcal{E}$) is a function of the velocity ($\dot{x}$):

$$\frac{\mathrm{d}\mathcal{E}}{\mathrm{d}t} = -C\dot{x}^2|\dot{x}|. \tag{6}$$

The total energy of our mechanical model without losses is $\mathcal{E} = \mathcal{T} + \mathcal{V}$. Differentiating $\mathcal{E}$ gives:

$$\frac{\mathrm{d}\mathcal{E}}{\mathrm{d}t} = \rho\mathcal{A}_{\text{c}}\dot{x}\left((x + L(1+\eta))\ddot{x} + \frac{\dot{x}^2}{2} + \frac{1}{\rho\mathcal{A}_{\text{c}}}\frac{\partial\mathcal{V}}{\partial x}\right); \tag{7}$$

it can be seen that the expression in brackets coincides with the equation of motion (4). We can assume that Eq. (4) is not strictly valid since losses are not equal to zero so that we can replace the expression in brackets with a generic loss term $\mathcal{G}(\dot{x})$. Equation (7) is transformed into:

$$\frac{\mathrm{d}\mathcal{E}}{\mathrm{d}t} = \rho\mathcal{A}_{\text{c}}\dot{x}\left(\mathcal{G}(\dot{x})\right). \tag{8}$$

Comparing this equation with (6), we conclude that $\mathcal{G}(\dot{x})$ is proportional to $\dot{x}|\dot{x}|$. This form agrees with the losses term that we proposed in (5) which shows that Lorenceau's results are equivalent to the form for the losses shown in (5).

Adding the nonlinear losses to Eq. (4), we obtain our basic model of the OWC dynamics:

$$(x + L(1+\eta))\ddot{x} + \frac{\dot{x}^2}{2} + \left(\frac{K}{2} + \frac{L}{D}f\right)\dot{x}|\dot{x}| + \frac{P_{\text{A}} - \rho g H}{\rho}\left(\left(1 - \frac{\mathcal{A}_{\text{c}} x}{V_0}\right)^{-\gamma} - 1\right) + gx = 0. \tag{9}$$

For small oscillations and assuming that $x \ll L$, we can discard the nonlinear terms such that the linear version of (9) can be rewritten as:

$$\ddot{x} + \omega_l^2 x = 0, \tag{10}$$

where ω_l is the natural frequency of oscillation of our system and this is defined by

$$\omega_l^2 = \gamma\frac{(P_{\text{A}} - \rho g H)\mathcal{A}_{\text{c}}}{\rho V_0 L(1+\eta)} + \frac{g}{L(1+\eta)}. \tag{11}$$

3 Parametric excitation

OWCs are normally excited externally by the waves which generate a periodic pressure signal at the lowest point of the duct. An alternative way to excite a mechanical model is by the periodic variation of one of the various parameters which describe the model. There are many parameters which are defined in the mechanical model of the OWC, some of which are involved in the definition of the natural frequency of oscillation (11). Our goal is to study the dynamics of the OWC when one of these parameters changes periodically in time in order to understand the conditions under which parametric resonance can occur.

Out of the parameters in (11), it appears that the most practical to vary periodically is the volume of the compression chamber. A simple implementation of this variation in volume can be described using Fig. 3. Here, the compresion chamber is also connected to a piston which is moving periodically.

The new arrangement is similar to an OWC device described in Sect. 2 but the oscillation of the piston modifies the volume in the compresion chamber. Including the movement of the piston in the adiabatic terms of Eq. (9) and assuming that the piston's displacement is periodic with amplitude b_p and frequency Ω, we may give the movement equation of the OWC by

$$(x+L(1+\eta))\,\ddot{x}+\frac{\dot{x}^2}{2}\left(\frac{K}{2}+\frac{L}{D}f\right)\dot{x}|\dot{x}|+\frac{P_\mathrm{A}-\rho gH}{\rho}\left(\left(1-\frac{\mathcal{A}_\mathrm{c}x+ab_\mathrm{p}\cos(\Omega t)}{V_0}\right)^{-\gamma}-1\right)+gx=0. \tag{12}$$

where a is the area of the piston.

The oscillation of the piston is a new way to supply energy to the OWC. Our goal is to study the dynamics of the oscillation of the water column due to the excitation produced by the piston movement.

Our first step is to expand Eq. (12) in terms of the periodic oscillation of the piston. In order to write Eq. (12) in nondimentional form, we perform the following changes of the variables, $\frac{\mathcal{A}_\mathrm{c}}{V_0}x\to x$ and $\hat{\omega}t\to t$:

$$\left(\frac{V_O}{L(1+\eta)\mathcal{A}_\mathrm{c}}x+1\right)\ddot{x}+\frac{V_0}{2L(1+\eta)\mathcal{A}_\mathrm{c}}\dot{x}^2+\frac{V_0}{L(1+\eta)\mathcal{A}_\mathrm{c}}\left(\frac{K}{2}+\frac{L}{D}f\right)\dot{x}|\dot{x}|$$
$$+\frac{(P_\mathrm{A}-\rho gH)\mathcal{A}_\mathrm{c}}{\hat{\omega}^2V_0L(1+\eta)\rho}\left(\left(1-x-\beta_\mathrm{p}\cos(\frac{\Omega}{\hat{\omega}}t)\right)^{-\gamma}-1\right)+\frac{g}{\hat{\omega}^2L(1+\eta)}x=0. \tag{13}$$

where $\beta_\mathrm{p}=\frac{ab_\mathrm{p}}{V_0}$ and $\hat{\omega}=\omega_\mathrm{I}$

We put a small perturbation β_p in our equation, where $|\beta_\mathrm{p}|\ll 1$. In the same way the amplitude of oscillation of the water column is assumed small; that is $|x|\ll 1$. We are interested in expanding the restitutive terms of the equation of motion which correspond to the last two terms of Eq. (12) in terms of the two small parameters, x and b_p. The main point of this study is to determine which terms of the expansion can produce resonance in the OWC since this is the most efficient mechanism to supply energy to the oscillation of the water column. The main terms of the expansion are:

– Linear terms:

$$\left[W+\frac{g}{L(1+\eta)\hat{\omega}^2}+\frac{(\gamma+1)(\gamma+2)W}{4}\beta_\mathrm{p}^2+(\gamma+1)W\beta_\mathrm{p}\cos\left(\frac{\Omega}{\hat{\omega}}t\right)\right.$$
$$\left.+\frac{(\gamma+1)(\gamma+2)W}{4}\beta_\mathrm{p}^2\cos\left(2\frac{\Omega}{\hat{\omega}}t\right)+\mathcal{O}(\beta_\mathrm{p}^3)\right]x, \tag{14}$$

where $W=\gamma\frac{(P_\mathrm{A}-\rho gH)\mathcal{A}_\mathrm{c}}{\hat{\omega}^2L(1+\eta)\rho V_0}$.

– Conservative nonlinear terms:

$$\frac{(\gamma+1)W}{2}x^2+\frac{(\gamma+1)(\gamma+2)W}{6}x^3+\mathcal{O}(x^4). \tag{15}$$

– Resonant forcing terms (we assume that $\left|\frac{\Omega}{\hat{\omega}}-1\right|\ll 1$ and $|W+\frac{g}{L(1+\eta)\hat{\omega}^2}-1|\ll 1$):

$$\left[W\beta_\mathrm{p}+\frac{(\gamma+1)(\gamma+2)W}{8}\beta_\mathrm{p}^3\quad+\mathcal{O}(\beta_\mathrm{p}^5)\right]\cos(\Omega t). \tag{16}$$

– Nonresonant forcing terms:

$$\frac{(\gamma+1)W}{4}\beta_{\mathrm{p}}^2+\frac{(\gamma+1)W}{4}\beta_{\mathrm{p}}^2\cos\left(2\frac{\Omega}{\hat{\omega}}t\right)+\frac{(\gamma+1)(\gamma+2)W}{24}\beta_{\mathrm{p}}^3\cos\left(3\frac{\Omega}{\hat{\omega}}t\right)+\mathcal{O}(\beta_{\mathrm{p}}^4). \tag{17}$$

The set of conservative nonlinear terms (15) in conjunction with the resonant forcing terms (16) behave similar to an OWC which is excited externally by the ocean waves. Studies of this kind of wave-energy device are described in [12] and [14]. In this paper we describe the effects of the nonlinearities on the dynamics of the OWC. Figure 4 shows a numerical integration of (13). The initial growth of the oscillation amplitude is modified until the amplitude becomes essentially constant after about 20 periods.

The first two linear terms in (14) are independent of β_{p}, followed by terms which depend on $\beta_{\mathrm{p}}, \cos(\frac{\Omega}{\hat{\omega}}t)$ and $\cos(2\frac{\Omega}{\hat{\omega}}t)$ up to order β_{p}^3. The linear frequency is modified by a small term which depends on β_{p}^2, thus producing an increase. The last two terms are multiplied by a periodic function. These terms are the main points of our study of the water-column oscillations, since they constitute a parametric excitation. We expect that the behavior of the attained amplitude of oscillation of Eq. (12), which is shown in Fig. 4, depends strongly on this excitation.

The mechanical implementation to produce parametric excitation in an OWC, which is shown in Fig. 3, combines two different phenomena: resonances which come from the forcing terms and parametric resonances due to the linear terms which include periodic variations of the main frequency of the water-column oscillation. We would now like to study the nonlinear effects of the mechanical oscillation due only to the parametric excitation. We thus do not want to include forcing terms in our model in order to obtain nonlinear solutions which come exclusively from the parametric phenomenon. In order to have a desired mechanical model of the OWC which only includes parametric excitations, we have to modify the external perturbation of the compression chamber. We would like to find a mechanism which produces periodic variations of the compression chamber volume V_0. The physical implementation of this kind of device is more complex than a simple piston because it is necessary to modify the amount of air which is contained in the chamber (the number of moles in the chamber). With this setup, the volume is perturbed in a periodical way: $V = V_0 + ab_{\mathrm{p}}\cos(\Omega t)$. The equation of motion of the OWC now becomes:

$$(x+L(1+\eta))\,\ddot{x}+\frac{\dot{x}^2}{2}+\left(\frac{K}{2}+\frac{L}{D}f\right)\dot{x}|\dot{x}|+\frac{P_{\mathrm{A}}-\rho gH}{\rho}\left(\left(1-\frac{\mathcal{A}_{\mathrm{c}}x}{V_0+ab_{\mathrm{p}}\cos(\Omega t)}\right)^{-\gamma}-1\right)+gx=0. \tag{18}$$

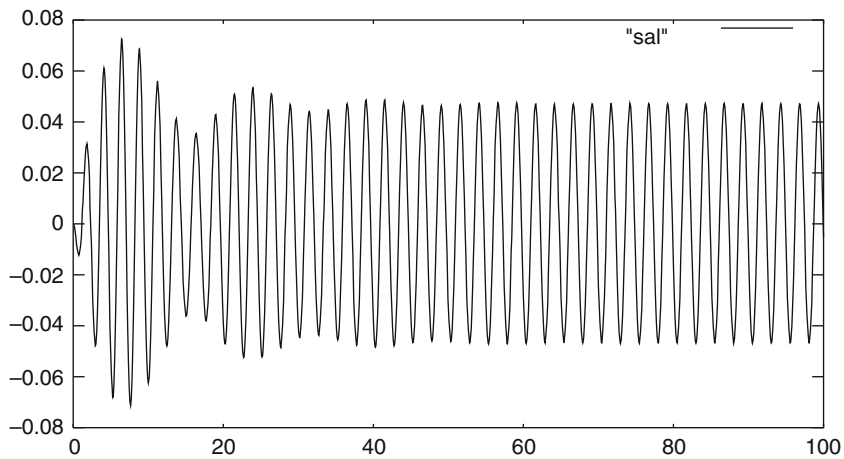

Fig. 4 Time evolution of the solution of Eq. (12). The vertical axis correspond to the amplitude of the oscillation

We proceed to analyze this equation similar to the previous case. The corresponding adimensional equation is the following:

$$\left(\frac{V_0}{L(1+\eta)\mathcal{A}_c}x+1\right)\ddot{x}+\frac{V_0}{2\mathcal{A}_c L(1+\eta)}\dot{x}^2+\frac{V_0}{\mathcal{A}_c L(1+\eta)}\left(\frac{K}{2}+\frac{L}{D}f\right)\dot{x}|\dot{x}| + \frac{(P_A-\rho gH)\mathcal{A}_c}{\hat{\omega}^2 V_0 L(1+\eta)\rho}\left(\left(1-\frac{x}{1+\beta_p\cos(\frac{\Omega}{\hat{\omega}}t)}\right)^{-\gamma}-1\right)+\frac{g}{\hat{\omega}^2 L(1+\eta)}x=0. \tag{19}$$

Let us suppose that x and β_p are very small in magnitude. Expanding the restitutive terms of Eq. (19) in terms of β_p and x, we obtain the main terms obtained are

– Linear terms:

$$\left[W+\frac{g}{\hat{\omega}^2 L(1+\eta)}+\frac{W}{2}\beta_p^2-W\beta_p\cos\left(\frac{\Omega}{\hat{\omega}}t\right)+\frac{W}{2}\beta_p^2\cos\left(2\frac{\Omega}{\hat{\omega}}t\right)+\mathcal{O}\left(\beta_p^3\right)\right]x. \tag{20}$$

– Conservative nonlinear terms are the same as Eq. (15) up to first order.

It is important to notice that there are no forcing terms in this expansion. Therefore, the volume perturbation that we introduced in Eq. (19) has parametric excitation exclusively. This model allows us to study the parametric excitation on an OWC alone.

A mechanical implementation of the periodic volume perturbation in the compression chamber is more complex than the perturbation with a simple piston attached to the compression chamber. A proposed mechanical device is described using Fig. 5. Here, the main compression chamber is connected to an adjacent volume of air by means of a valve. When this valve is open, the total volume of air increases, softening the air-spring restoring force. In this way, opening and closing the air valve modifies the air-spring constant, thereby changing one of the parameters of the system. The piston shown in Fig. 5 would be used to modify the equilibrium level of the water-column surface to compensate for variations produced by the valve.

In Fig. 6, a full cycle of oscillation is shown as an aid to describe one way in which parametric resonance could be induced using the device shown in Fig. 5. The cycle is divided into four sections as follows. In the first quarter, that is, when the water level descends from (I) before reaching the equilibrium level at (II), the air valve in Fig. 5 is closed so that the spring is harder, forcing the water column down faster than if the valve were open. Nevertheless, closing the valve at the highest point (I), raises the equilibrium level of the water-column surface to point A, above the reference level at point B. In order to take advantage of the increased potential energy of the hardened spring, we must restore the equilibrium level during this part of the cycle, to reference point B, by pushing the piston (P) in Fig. 5, an appropriate displacement. By doing this, the kinetic energy of the system, when the water level reaches (II), will be greater than if the valve had been left open, at the expense of the work performed by the piston. It must be noted that the work done by the piston corresponds to the energy supplied to the mechanical system.

In the next quarter cycle, that is, from (II) to (III), the valve is now opened to soften the air spring, so that the kinetic energy at point II will transform into a greater displacement at point III. Opening the valve at point II, however, lowers the equilibrium level to point C so that the piston must be extracted to restore this point to B.

During the remaining two quarter-cycles, that is from (III) to (IV) and from (IV) to (V), the air valve and the piston are operated in a similar way. The aim is to harden the air spring when the speed of the water column is increasing and soften it when the speed is decreasing. External work is done by pushing and pulling the piston, in order to keep the average equilibrium level fixed.

When the spring is soft, the natural frequency of oscillation can be defined as ω^- which is smaller than ω_0 by a certain $\Delta\omega$, which depends on the relative size of the two air chambers connected by the valve. In a similar way, when the spring is hard, the corresponding frequency is ω^+. When the process described in the previous two paragraphs is followed, it can be shown that the oscillation amplitude will increase by

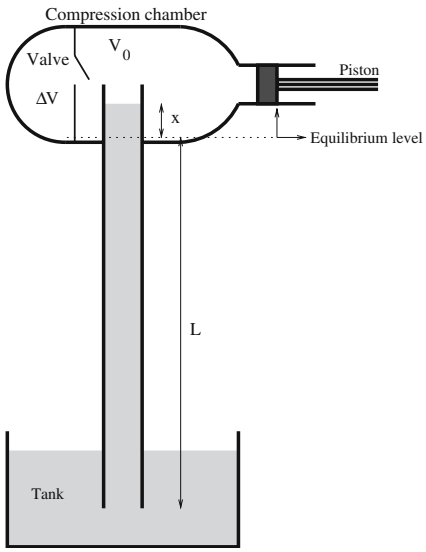

Fig. 5 Possible implementation of a parametric excitation of an OWC. The volume of the compression chamber is changed by the action of the piston and the valve

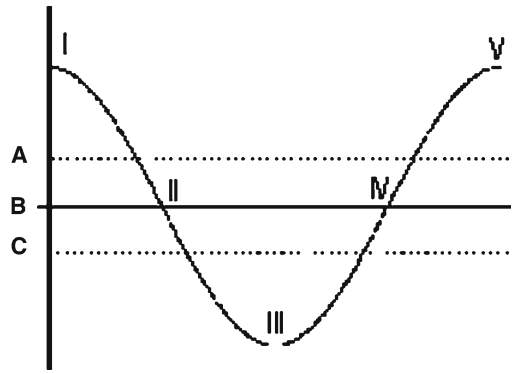

Fig. 6 Water level of the oscillating water column versus time. Point B represents the reference level

$(\omega^+/\omega^-)^2 > 1$ from cycle to cycle. That is, the increase is proportional to the amplitude of the previous cycle so that there is an exponential increase in time. It is clear that the energy required by the mechanical system to increase the amplitude of the oscillation comes from the work performed by the piston. The piston injects energy to our system two times every cycle. Parametric resonance is an optimal way to supply energy to any system because all this energy is used to increase the kinetic energy of the mechanical system.

In the next section we study the mechanical response of the water column when we only consider the linear term of Eq. (18), in which case the linear frequency is modified in a periodic way. This kind of phenomenon is studied by Floquet theory.

The nonlinear terms limit the growth of the amplitude of oscillation to a maximum value. The main goal of our task is to determine how this maximum value depends on the nonlinear terms of Eq. (18). The next section is devoted to examining the main features of the parametric resonance in the linear case. In Sects. 5 and 6 we study the effect of other nonlinear terms on parametric resonance.

4 Linear approximation and the Floquet method

In this section we simplify the mechanical model of the OWC such that we only take into account the linear terms in $x, \dot{x}$ and $\ddot{x}$. Using the linear part of Eq. (19) (where we take only into account the first harmonic of Eq. (20)) we obtain a simple differential equation for the dynamics of the water column:

$$\ddot{x} + \left[W + \frac{g}{\hat{\omega}^2 L(1+\eta)} + \frac{W}{2}\beta_{\mathrm{p}}^2 - W\beta_{\mathrm{p}} \cos\left(\frac{\Omega}{\hat{\omega}} t\right) \right] x = 0. \tag{21}$$

It is possible to simplify the previous equation, by defining

$$\omega_0^2 = W + \frac{g}{\hat{\omega}^2 L(1+\eta)} + \frac{W}{2}\beta_{\mathrm{p}}^2 \tag{22}$$

and

$$\beta = -W\beta_{\mathrm{p}},$$

where $\hat{\omega}^2(W + \frac{g}{\hat{\omega}^2 L(1+\eta)})$ corresponds to the natural frequency (11) of (9) for small oscillations. Then, Eq. (21) can be written like Mathieu's equation:

$$\ddot{x} + \left(\omega_0^2 + \beta \cos\left(\frac{\Omega}{\omega_0} t\right)\right) x = 0, \tag{23}$$

The solution of this equation can be obtained through the Floquet theory [17]. It is well known that the solution of this equation is the product of a periodic function with period $2\pi\omega_0/\Omega$ and an exponential function. Using Floquet theory, the form of the parameter which appears in the argument of the exponential function can be found. For a real parameter, the solution grows exponentially in time so that the solution is unbounded. This case corresponds to the parametric resonant condition. The other possibility is when the parameter is an imaginary number; in that case the solution is bounded because it is the product of two periodic functions. The behavior of the solution is independent of the initial conditions of the linear differential equation (23). The main problem is to determine the form of the parameter in the argument of the exponential function, which is a function of β and $(\omega_0/\Omega)^2$. Using standard asymptotic methods, described in [18, pp. 267–294], we can find the bifurcation diagram which determines the stability of the solution, this diagram is shown in Fig. 7. The darkened areas in the figure cover the values of ω_0/Ω and β where the solutions to Mathieu's equation grow exponentially in time. These regions, which grow thin when β goes to zero, are known as Arnold's tongues. We have an infinite number of these regions of instability, each region departing from one point of the line $\beta = 0$. These points are located at $(\omega_0/\Omega)^2 = (n/2)^2$, for $n = 0, 1, 2, \ldots$. These regions define the parametric resonance of Mathieu's equation and the main tongue of the bifurcation diagram, shown in Fig. 7, corresponds to values of Ω close to $2\omega_0$. The frequency of the parametric perturbation must belong to the interval $\Omega \in (2\omega_0 - \beta/2, 2\omega_0 + \beta/2)$ for small values of β [18, pp. 267–294]. As β grows, the region where parametric resonance occurs increases, as can be seen in Fig. 7. This is a useful property because precise tuning to the resonant frequency is not needed in order to obtain an unbounded solution of Mathieu's equation.

Physically we cannot expect the oscillation of the water column to grow indefinitely in time since the nonlinear terms of the full equation (18) will limit growth to a maximum amplitude of oscillation. Figure 8 shows a numerical integration of (18). The oscillation of the water column, perturbed by a parametric excitation in the volume of the compression chamber, can be seen initially to grow exponentially with time, starting from a small oscillation. After a certain point, growth is curbed until the oscillation reaches a constant amplitude due to the nonlinear losses; in this case the energy that we supply to the system is equal to the nonlinear losses.

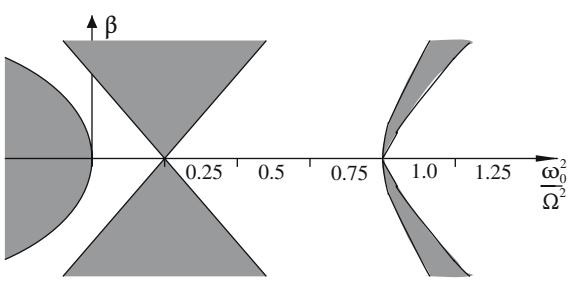

Fig. 7 Bifurcation diagram of Mathieu's equation. The darked areas correspond to a unbounded solutions

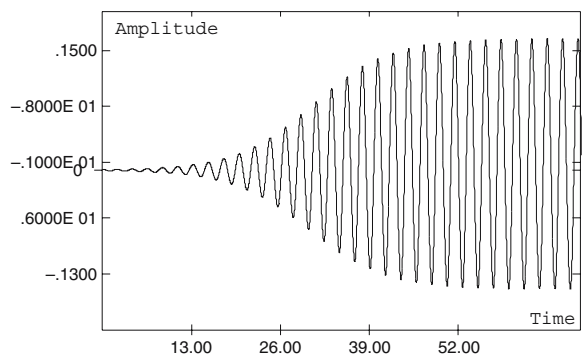

Fig. 8 Time evolution of the solution of Eq. (18). The vertical axis correspond to the amplitude of the oscillation

5 Asymptotic study of a nonlinear oscillation

The purpose of this section is to study the properties of the nonlinear solution of the full equation (18) under parametric resonance. As before, the parametric excitation is produced by a periodic variation of the volume of the compression chamber using the piston and the set of valves as shown in Fig. 5. The nonlinear terms of Eq. (18) come from the nonlinear losses (5) and the adiabatic compression term (4). In order to simplify the study of our full equation, we rewrite Eq. (18) by expanding in third-order Taylor series and grouping terms:

$$\ddot{x} + \epsilon\zeta\dot{x}^2 + \big(\omega_0^2 + \epsilon\cos(\Omega t)\big)x + \epsilon\alpha x^2 + \epsilon\beta x^3 + \epsilon\kappa\dot{x}|\dot{x}| = 0, \tag{24}$$

where ω_0 is defined in (22), $\epsilon, \epsilon\alpha x^2$ and $\epsilon\beta x^3$ are defined as follows:

$$\epsilon\alpha = C\frac{\mathcal{A}_c^2}{2V_0^2}(\gamma^2+\gamma), \quad \epsilon\beta = C\frac{\mathcal{A}_c^3}{6V_0^3\epsilon}(\gamma^3+3\gamma^2+2\gamma),$$
$$\epsilon\zeta = \frac{1}{2L(1+\eta)} \quad \epsilon = C\frac{\gamma\mathcal{A}_c}{V_0}b_p, \quad C = \frac{P_A - \rho g H}{\rho L(1+\eta)}. \tag{25}$$

The losses are represented by the parameters $\epsilon\kappa = \frac{1}{L(1+\eta)}(\frac{K}{2} + \frac{L}{D}f)$. In order to perform an asymptotic study of Eq. (24), we scale the nonlinear terms with the small parameter ϵ; the parametric perturbation is also scaled with this small parameter. It is a standard procedure in mathematics to homogenize the order of the nonlinear terms so that we can carry out asymptotic calculations in terms of a small parameter ϵ.

In order to simplify the study of Eq. (24), we split the problem in two parts. In the first one, only the nonlinear terms, which come from the adiabatic compression term, are considered. In the second case, we only consider the nonlinear terms related to the losses of the system. In both cases we include the parametric excitation and our goal is to find the size of the attainable growth of amplitude of the asymptotic solution. In both cases we use the Multiple Scale Method. For good references of this method see [19, Chapter 4], [20, Chapter 6], and [21, Chapter 9].

5.1 Case 1: Adiabatic compression

Equation (24) is reduced to the following form when nonlinear losses are disregarded:

$$\ddot{x} + \epsilon\zeta\dot{x}^2 + \big(\omega_0^2 + \epsilon\cos(\Omega t)\big)x + \epsilon\alpha x^2 + \epsilon\beta x^3 = 0. \tag{26}$$

We are interested in finding solutions close to parametric resonance, when the parametric excitation frequency is close to $2\omega_0$. From Floquet theory, this means that Ω should be within the main Arnold's tongue.

The Multiple Scale Method is an asymptotic procedure which considers that nonlinear dynamics take place on a longer time scale than $2\pi/\omega_0^2$. This method considers a set of time variables $\{t_i\}$ which are related by the small parameter ϵ in this form: $t_i = \frac{1}{\epsilon}t_{i+1}$, for $i = 0, 1, 2, \ldots$ The first time scale, t_0, corresponds to the period of one oscillation of Eq. (23). The scale t_1 corresponds to a larger period of time when it is possible to detect modulation phenomena of the nonlinear equation, etc. Because this method works in multiple time scales, the solution of (26) should be a sum of terms which correspond to solutions at different time scales:

$$x = x_0(t_0, t_1, \ldots) + \epsilon x_1(t_0, t_1, \ldots) + \epsilon^2 x_2(t_0, t_1, \ldots) + \cdots. \tag{27}$$

It is important to remark that each term of this sum is a function of the set of time variables $\{t_i\}$. In nonlinear dynamics, the frequency of the solution is usually a function of the amplitude of the perturbation. Thus it is reasonable to write the frequency of the solution as a power series of the perturbation parameter:

$$\omega^2 = \omega_0^2 + \epsilon\omega_1^2 + \epsilon^2\omega_2^2 + \cdots. \tag{28}$$

In this problem we have taken into account a set of time variables. In order to solve the differential equation, it is necessary to redefine the differential operator which can be written in this form:

$$D = D_0 + \epsilon D_1 + \epsilon^2 D_2 + \epsilon^3 D_3 + \cdots, \tag{29}$$

where $D_i = \frac{\mathrm{d}}{\mathrm{d}t_i}$, for $i = 0, 1, 2, \ldots$.

Now, we can compute the first and the second derivatives of function (27) using the definition of the differential operator:

$$\begin{aligned} \dot{x} &= D^1 x = D_0 x_0 + \epsilon(D_1 x_0 + D_0 x_1) + \epsilon^2(D_2 x_0 + D_1 x_1 + D_0 x_2) + \cdots, \\ \ddot{x} &= D^2 x = D_0^2 x_0 + \epsilon(D_0^2 x_1 + 2D_1 D_0 x_0) + \epsilon^2(D_0^2 x_2 + 2D_1 D_0 x_1 + 2D_2 D_0 x_0 + D_1^2 x_0) + \cdots, \end{aligned} \tag{30}$$

where $D_k^j x_i = \frac{\mathrm{d}^j x_i}{\mathrm{d}t_k^j}$, for $i, j, k = 0, 1, 2, \ldots$.

The other terms of Eq. (26) can be written in terms of the proposed solutions (27) and (28):

$$\begin{aligned} \omega^2 x &= \omega_0^2 x_0 + \epsilon\left(\omega_0^2 x_1 + \omega_1^2 x_0\right) + \epsilon^2\left(\omega_0^2 x_2 + \omega_1^2 x_1 + \omega_2^2 x_0\right) + \cdots, \\ x^2 &= x_0^2 + 2\epsilon x_0 x_1 + \epsilon^2\left(x_1^2 + 2x_0 x_2\right) + \cdots, \\ x^3 &= x_0^3 + 3\epsilon x_0^2 x_1 + \cdots. \end{aligned} \tag{31}$$

The next step is to take all the terms defined in Eqs. (30), (31) and substitute them in Eq. (26). We obtain an infinite number of terms but they can be grouped in terms of powers of the small parameter ϵ. In this way we obtain a set of an infinite number of linear differential equations:

$$\epsilon^0 : \; D_0^2 x_0 + \omega_0^2 x_0 = 0, \tag{32a}$$

$$\epsilon^1 : D_0^2 x_1 + \omega_0^2 x_1 = -\omega_1^2 x_0 - 2D_1 D_0 x_0 - \alpha x_0^2 - \beta x_0^3 - \zeta (D_0 x_0)^2 - \cos(2\omega_0 t_0) x_0, \tag{32b}$$

$$\begin{aligned} \epsilon^2 : D_0^2 x_2 + \omega_0^2 x_2 = {} & -\omega_2^2 x_0 - \omega_1^2 x_1 - 2D_1 D_0 x_1 - 2D_2 D_0 x_0 - 2\alpha x_0 x_1 - 3\beta x_0^2 x_1 \\ & - \cos(2\omega_0 t_0) x_1 - D_1^2 x_0 - 2\zeta D_0 x_0 (D_1 x_0 + D_0 x_1), \end{aligned} \tag{32c}$$

$$\begin{array}{l} . \\ . \\ . \\ . \end{array}$$

The corresponding differential equation of order ϵ^k is a linear equation in x_k, the terms on the right-hand side of this equation depending on the functions $x_0, x_1, \ldots, x_{k-1}$ which have been solved in the previous steps; these solutions are functions of the time variables $t_0, t_1, \ldots, t_{k-1}$. Therefore, we have an inhomogeneous linear differential equation for x_k.

We start by solving the first equation of order ϵ^0. Let $x_0(t_0)$ be the solution of Eq. (32a); then the form of this solution is

$$x_0(t) = A \sin(\omega_0 t_0) + B \cos(\omega_0 t_0), \tag{33}$$

where A and B are functions of the "slow times" $t_1, t_2, \ldots$. We are able to solve Eq. (32b) because the right-side terms of this equation are only functions of the time variables t_0 and t_1. Replacing Eq. (33) in 32b, we obtain the following linear differential equation:

$$\begin{aligned} D_0^2 x_1 + \omega_0^2 x_1 = {} & \sin(\omega_0 t_0)\left[-\omega_1^2 A + 2\omega_0 D_1 B - \frac{3}{4}\beta A^3 - \frac{3}{4}\beta A B^2 + \frac{1}{2}A\right] \\ & + \cos(\omega_0 t_0)\left[-\omega_1^2 B - 2\omega_0 D_1 A - \frac{3}{4}\beta A^2 B - \frac{3}{4}\beta B^3 - \frac{1}{2}B\right] \\ & + \sin(2\omega_0 t_0)\left[-\alpha A B - \zeta \omega_0^2 A B\right] \\ & + \cos(2\omega_0 t_0)\left[\frac{\alpha}{2}A^2 + \frac{\alpha}{2}B^2 - 1 - \frac{\zeta}{2}\omega_0^2 (B^2 - A^2)\right] \end{aligned}$$

$$
\begin{aligned}
&+\sin(3\omega_0 t_0)\left[-\frac{\beta}{4}A^3-\frac{3}{4}\beta AB^2-\frac{1}{2}A\right]\\
&+\cos(3\omega_0 t_0)\left[-\frac{3}{4}\beta A^2B-\frac{\beta}{4}B^3-\frac{1}{2}B\right]\\
&+\left[-\frac{\alpha}{2}A^2-\frac{\alpha}{2}B^2-\frac{\zeta}{2}\omega_0^2(A^2+B^2)\right].
\end{aligned}
\tag{34}
$$

In this case, we must consider that A and B are functions of the "slow time" t_1, such that D_1A and D_1B are the derivatives of these functions with respect to the "slow time" t_1.

The Multiple Scale Method requires that the set of solutions $x_i(t_0, t_1, \ldots)$ must be bounded in time. In order to achieve this, the terms which depend on $\sin(\omega_0 t_0)$ and $\cos(\omega_0 t_0)$, which are resonant, must be eliminated by setting their coefficients to zero. In this form, we obtain two differential equations for the amplitudes $A(t_1)$ and $B(t_1)$:

$$
\begin{aligned}
2\omega_0 D_1 A &= -\left(\frac{1}{2}+\omega_1^2\right)B-\frac{3}{4}\beta B(A^2+B^2),\\
2\omega_0 D_1 B &= \left(-\frac{1}{2}+\omega_1^2\right)A+\frac{3}{4}\beta A(A^2+B^2).
\end{aligned}
\tag{35}
$$

In order to simplify the study of these nonlinear differential equations, we introduce the change of variables $A(t_1) = r(t_1)\cos(\theta(t_1))$ and $B(t_1) = r(t_1)\sin(\theta(t_1))$:

$$
\begin{aligned}
2\omega_0 D_1 r &= -\frac{r}{2}\sin(2\theta),\\
2\omega_0 r D_1\theta &= \omega_1^2 r-\frac{r}{2}\cos(2\theta)+\frac{3}{4}\beta r^3.
\end{aligned}
\tag{36}
$$

We do not have to solve Eq. (36) because we are interested in finding the asymptotic behavior of the amplitudes A and B. The dynamical evolution of these amplitudes can be determined by the limit sets of Eq. (36). In this case, the limit sets correspond to the set of fixed points of (36), these points can be found by equating to zero the right-side terms of Eq. (36). The set of fixed points are the following:

$$
\theta = n\pi \quad r = \pm\sqrt{\frac{2}{3\beta}}\sqrt{1-2\omega_1^2} \quad \text{or} \quad r = 0,
\tag{37}
$$

where $n = 0, 1$.

In order to obtain the linear stability of the fixed points, it is necessary to evaluate the Jacobian matrix at those points:

$$
DF = \begin{pmatrix} 0 & \pm\frac{1}{2\omega_0}\sqrt{\frac{2}{3\beta}}\sqrt{1-2\omega_1^2} \\ \frac{3}{4\omega_0}\beta\sqrt{\frac{2}{3\beta}}\sqrt{1-2\omega_1^2} & 0 \end{pmatrix}.
\tag{38}
$$

The corresponding eigenvalues of the fixed points are $\lambda^2 = \pm(1-2\omega_1^2)/(4\omega_0^2)$. We have two elliptic fixed points and one hyperbolic point. The origin is a hyperbolic point and there are two elliptic points located at both sides of the origin. The elliptic points are equidistant to the origin where the hyperbolic point is located. Figure 9 shows the phase space of Eq. (36).

For small initial values of A and B, we can observe that these functions have a periodic behavior; the corresponding frequency of these functions is close to the eigenvalue of the elliptic point. The period is then close to

$$
T = \frac{4\pi}{\epsilon}\frac{\omega_0}{\sqrt{1-2\omega_1^2}}.
\tag{39}
$$

It is clear that the functions A and B have a longer period than the first-order solution $x_0(t_0)$; the oscillatory solution of (32a) is modulated by the amplitudes $A(t_1)$ and $B(t_1)$. The maximum attainable oscillatory amplitude is then given by

$$A_{\max}(\beta,\omega_1)=\sqrt{\frac{2}{3\beta}}\sqrt{1-2\omega_1^2}. \tag{40}$$

A similar expression can be obtained for $B_{\max}$. It is worth noting that the maximum amplitude of the oscillation is inversely proportional to the square root of the perturbation amplitude. $A_{\max}$ is also proportional to $\sqrt{1-2\omega_1^2}$, the behavior of the amplitude with respect to the tuning parameter ω_1. We can determine how the amplitude decreases by a small shift of the frequency with respect to the main parametric resonance $2\omega_0$. When $2\omega^2 > 1$, the solution of the nonlinear equation (26) falls outside the main Arnold's tongue such that the solution does not grow exponentially in time.

5.2 Case 2: Nonlinear losses

In previous works we have studied the effect of the nonlinear terms in the sea-water-pump equations [12, 14]. We found that vortex formation and radiation damping are the main losses of our system; these losses are included in the term $\epsilon\kappa\dot{x}|\dot{x}|$ in Eq. (24). In order to study the effect of this term, we perturb Mathieu's equation by including it. Our differential equation is now:

$$\ddot{x}+\epsilon\zeta\dot{x}^2+\left(\omega_0^2+\epsilon\cos(\Omega t)\right)x+\epsilon\kappa\dot{x}|\dot{x}|=0. \tag{41}$$

Similar to our previous case, we apply the Multiple Scale Method to obtain an asymptotic solution of Eq. (41) such that we are able to compute the maximum amplitude of oscillation. The asymptotic method cannot be directly applied to Eq. (41) because we cannot take the derivatives of $|\dot{x}|$ close to zero. Nevertheless, we can replace the losses term $\dot{x}|\dot{x}|$ by an analytic function which resembles closely the shape of the graph of $\dot{x}|\dot{x}|$. Using the following identity $\dot{x}|\dot{x}|=\dot{x}^3/|\dot{x}|$ and considering that

$$\dot{x}\sim\dot{x}_0=\omega_0\left(A\cos(\omega_0 t_0)-B\sin(\omega_0 t_0)\right),$$

where x_0 is the solution of (32a), we have the following approximation:

$$\dot{x}|\dot{x}|\sim\frac{\dot{x}^3}{\omega_0\sqrt{A^2+B^2}}. \tag{42}$$

Up to now, our nonlinear differential equation is

$$\ddot{x}+\epsilon\zeta\dot{x}^2+\left(\omega_0^2+\epsilon\cos(\Omega t)\right)x+\epsilon\kappa\frac{\dot{x}^3}{\omega_0\sqrt{A^2+B^2}}=0. \tag{43}$$

We are interested in obtaining an approximate solution when the parametric excitation is at resonance, $\Omega=2\omega_0$. We apply again the Multiple Scale Method to our Eq. (43) such that we can proceed similar to case 1: in this case Eq. (43) is worked out similar to Eq. (26) such that we obtain similar equations from (27) to (34).

The corresponding equation to (35) is now

$$\begin{aligned}2\omega_0 D_1 A&=-\left(\frac{1}{2}+\omega_1^2\right)B-\frac{3}{4}\kappa\omega_0^2 A(A^2+B^2)^{1/2},\\ 2\omega_0 D_1 B&=\left(-\frac{1}{2}+\omega_1^2\right)A-\frac{3}{4}\kappa\omega_0^2 B(A^2+B^2)^{1/2}.\end{aligned} \tag{44}$$

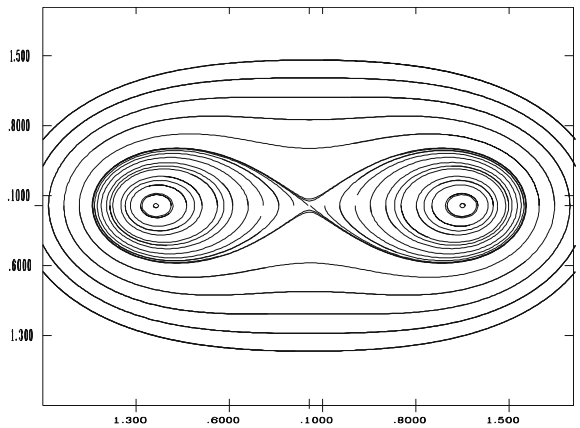

Fig. 9 Phase space of the solution of Eq. (36)

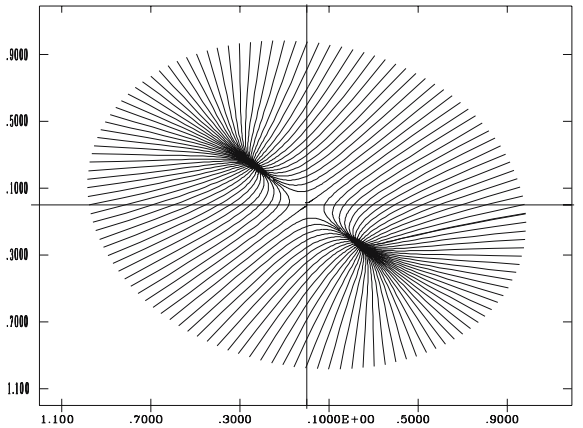

Fig. 10 Phase space of the solution of Eq. (45). Two global attractor points can be readily identified

In order to simplify our study of Eq. (44), we carry out the change of variables $A(t_1) = r(t_1)\cos(\theta(t_1))$ and $B(t_1) = r(t_1)\sin(\theta(t_1))$:

$$2\omega_0 D_1 r = -\frac{r}{2}\sin(2\theta) - \frac{3}{4}\kappa\omega_0^2 r^2,$$
$$2\omega_0 r D_1\theta = \omega_1^2 r - \frac{r}{2}\cos(2\theta). \tag{45}$$

It is not necessary to solve Eq. (45), we only need to obtain the asymptotic behavior of $r(t_1)$ and $\theta(t_1)$ in order to estimate the attainable amplitude in the steady state. The set of fixed points of (45) can be obtained by setting $\omega_1^2 - \frac{1}{2}\cos(2\theta) = 0$; then $\sin(2\theta) = \pm\sqrt{1 - \left(2\omega_1^2\right)^2}$. Therefore, the fixed points are the following:

$$r = \pm\frac{2}{3\kappa\omega_0^2}\sqrt{1 - 4\omega_1^4} \quad \text{and} \quad r = 0. \tag{46}$$

We have three fixed points. Using the Jacobian matrix we can obtain the linear stability of this set of fixed points. The eigenvalues of the two fixed points different to the origin are $\lambda_1 = 0$ and $\lambda_2 = -\frac{13}{2}\sqrt{1 - 4\omega_1^4}$. These points have a central manifold [22, pp. 117–138] but the phase space shows that they behave like attractors (Fig. 10 shows the phase space). The origin is a saddle point.

It is noteworthy that there are two attractor points in Fig. 10, which means that any initial conditions evolve towards one of these points. The maximum attainable amplitude of Eq. (41) is

$$A_{\max}(\kappa, \omega_1) = \frac{2}{3\kappa\omega_0^2}\sqrt{1 - 4\omega_1^4}. \tag{47}$$

In this case, the solution does not exhibit a modulation phenomenon because A and B evolve to an attractor in the "long-time" regime. Another fact is that the attainable amplitude is proportional to the inverse of the coefficient κ. In contrast, in case 1 the maximum amplitude increases like the inverse of the square root of β.

The solution of Eq. (41) grows exponentially at first until it reaches the maximum attainable amplitude. The solution then keeps this amplitude without modulation. The maximum amplitude depends on the factor $\sqrt{1 - 4\omega_1^4}$; this term determines the amplitude of the solution when the parametric excitation differs from the resonant condition $\Omega = 2\omega_0$. The parameter ω_1 is the tuning term. As in the previous case, we have parametric resonance if $2\omega_1^2 < 1$. This solution belongs to the main Arnold's tongue. For small

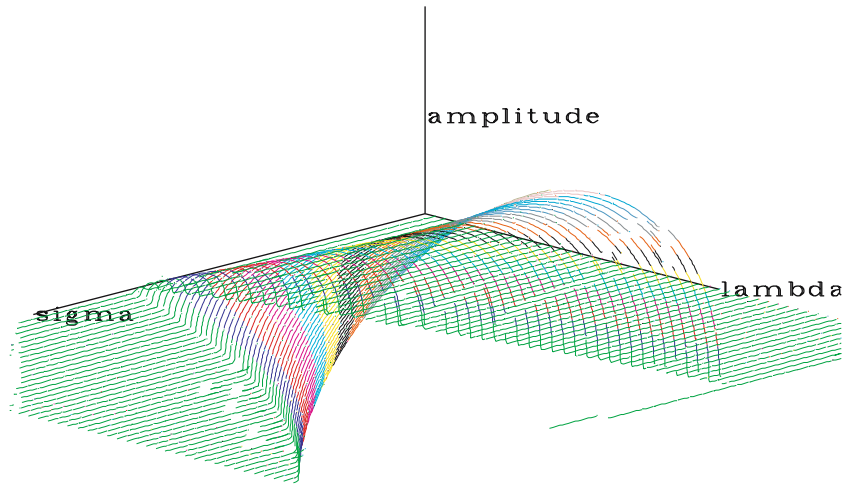

Fig. 11 Three dimensional representation of the solution of Eq. (18) where the parametric excitation is given by (48). The vertical axis represents the maximum amplitude of the numerical solution for fixed values of λ and σ. The ranges of λ and σ are $[0, 0{\cdot}5]$ and $[1{\cdot}7, 2{\cdot}2]$ respectively. The amplitude ranges from 0 to 0·25

values of the de-tuning parameter ω_1, the variation of the amplitude is negligible because ω_1^4 is too small. A three-dimensional drawing of this Arnold's tongue is shown in Fig. 11 (where *sigma* is the de-tuning parameter and *lambda* is the magnitude of the perturbation term $\frac{2}{3\kappa\omega_0^2}$).

6 Numerical experiments

The asymptotic method is a powerful tool to understand the quantitative dynamics of the mechanical systems in which we are interested. The last section was devoted to obtaining the maximum attainable amplitude of oscillation of a water column which has an air-compression chamber at the top of the duct. The water column is excited by a periodic variation of one of the system parameters. The nonlinear terms bound the amplitude of oscillation of the OWC.

We are interested in verifying the accuracy of the asymptotic methods that were developed in the previous section. Our goal is to determine the maximum amplitude of oscillation by numerically simulating the dynamics of the OWC with parametric excitation when the volume of air in the compression chamber is modified periodically with a valve and piston. We solve the differential equation (18) using a numerical procedure. We expect to obtain, at the starting point of our simulation, an exponential growth of the oscillation's amplitude since the nonlinear terms are small and the behavior of the differential equation is essentially linear. After a certain period of time, the numerical solution should reach a maximum amplitude defined by the nonlinear terms.

We are interested in studying the behavior of the numerical solution for a set of values of the frequency and amplitude of the parametric excitation in our model. For any pair of frequency and amplitude values, we obtain a numerical solution of Eq. (18) for a long period of time from which we can compute the maximum amplitude of oscillation. Using this information we are able to compare the numerical and asymptotic values of the attainable growth of the amplitude.

In order to define the value of the parameters which are involved in our differential equation (18), we resort to the numerical model of a 1:25 scale wave-driven sea-water pump as described in [12, 14]. Table 1 shows the values that we use in our numerical simulation. We must remark that the set of data in Table 1 corresponds to a real experiment with a scale-model of a wave-driven sea-water pump tested in a wave tank.

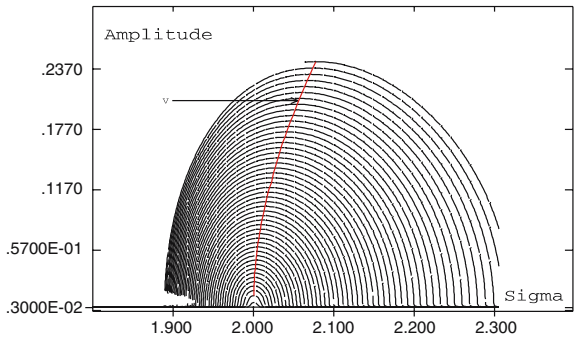

Fig. 12 Maximum amplitude of oscillation of the solution of Eq. (18) versus σ. Each curve is obtained for a fixed value of λ. Curve V joins the maximum values of each curve

Table 1 Parameter values

$\mathcal{A}_c = 0{\cdot}002463\,\mathrm{m}^2$	$a = 0{\cdot}001130\,\mathrm{m}^2$
$\gamma = 1{\cdot}4$	$f_r = 0{\cdot}06064$
$L = 4{\cdot}325\,\mathrm{m}$	$K = 0{\cdot}1$
$\frac{K}{2} + \frac{L}{D} f_r = 4{\cdot}4683$	$V_0 = 0{\cdot}011583\,\mathrm{m}^3$
$\omega_0 = 2{\cdot}7902\,\frac{1}{\mathrm{s}}$	$H = 1{\cdot}26\,\mathrm{m}$
$\frac{P_A - \rho g H}{\rho} = 88{\cdot}961\,\mathrm{m}^2/\mathrm{s}^2$	

The volume of the compression chamber is varied periodically in time as

$$V = V_0\,(1 + \lambda \cos(\sigma \omega_0 t))\,, \tag{48}$$

where λ is the amplitude of the parametric perturbation; this parameter represents the ratio $\Delta V_0/V_0$. The parameter σ represents the tuning respect to the natural oscillation frequency of the OWC, ω_0, where $\sigma\omega_0$ is the frequency of the parametric excitation.

We are interested in computing the maximum amplitude of the numerical solution of (18) for values of σ close to 2, which corresponds to the parametric resonance in the linear model. We use a Runge-Kutta method of order 7–8 to solve the differential equation (18); this routine has a variable step in time. For each value of σ and λ, we compute the numerical solution of (18), with a simulation time of 500 units. The maximum time step of the integration routine is 0·2. We set a maximum error for each step of integration as 10^{-11}. The initial conditions are set to the values, $x_0 = 0{\cdot}0001$ and $\dot{x}_0 = 0$.

The set of values of λ and σ that we use in our numerical experiment belong to the following intervals:

$$\sigma \in (1{\cdot}7, 2{\cdot}2), \quad \lambda \in (0{\cdot}01, 0{\cdot}5), \tag{49}$$

where the step size of λ is 10^{-4} and for σ is 10^{-2}. Thus, we performed 250,000 numerical simulations of our differential equation. The computations were made with a cluster of 34 Pentium processors at 800 MHz. The solutions of this experiment are shown in Fig. 11, where the vertical axis corresponds to the maximum attained oscillation amplitude for each pair of values σ and λ. This figure looks like a three-dimensional Arnold's tongue.

We can plot the amplitude of the oscillation versus the value of the excitation frequency (Fig. 12). Each curve has a fixed value of the perturbation parameter λ. The line crossing the said curves joins their maximum values.

The main interest of this section is to compare the asymptotic estimation obtained in the previous section to the numerical results in Figs. 11 and 12. First, we must define the value of the parameters which appear in Eq. (24) in terms of the value of the parameters shown in Table 1.

Our first step is to expand the adiabatic term in a power series (4) with respect to the variable $\mathcal{A}_c/V_0$. We only need to take into account terms up to order three. Because the volume appears in the denominator of the natural oscillation frequency (11), we must replace the volume by the expression shown in Eq. (48). In this form we can expand the volume in a Taylor series with respect to the small parameter λ. After that, we are able to write the corresponding differential equation of the water-column oscillations using the data of the real experiment given in Table 1:

$$\ddot{x} + 0{\cdot}11347\dot{x}^2 + 1{\cdot}03315\dot{x}|\dot{x}| + \left(8{\cdot}391 + 2{\cdot}918\lambda^2 + 5{\cdot}978\lambda\cos(\sigma\omega_0 t)\right) x + 1{\cdot}56247x^2 + 0{\cdot}37654x^3 = 0. \tag{50}$$

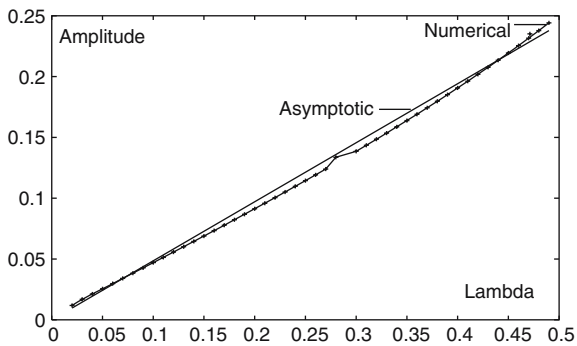

Fig. 13 Amplitudes from curve V in Fig. 9 versus λ (—+——+—). Asymptotic estimate of the amplitude A_κ given in (52) (————)

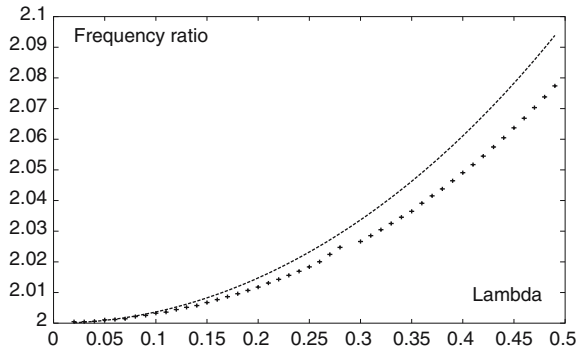

Fig. 14 $\Omega/\hat{\omega}_0(\lambda)$ plotted against λ. The solid line is the graph of Eq. (53). The dots correspond to curve V shown in Fig. 12

Equation (50) is similar to Eq. (24). Comparing the linear terms in both equations we get that $\omega_0^2 = 8{\cdot}391 + 2{\cdot}918\lambda^2$ and $\epsilon\cos(\Omega t) = 5{\cdot}978\lambda\cos(\sigma\omega_0 t)$. In this form, the small parameters λ and ϵ are related in the following way, $\epsilon = 5{\cdot}978\lambda$. It follows that the coefficients of the nonlinear terms are related as $\epsilon\alpha = 1{\cdot}56247, \epsilon\beta = 0{\cdot}37654$ and $\epsilon\kappa = 1{\cdot}03315$. Replacing ϵ in these relations, we obtain

$$\begin{aligned} \kappa &= 0{\cdot}1728\lambda^{-1}, \\ \alpha &= 0{\cdot}2613\lambda^{-1}, \\ \beta &= 0{\cdot}0629\lambda^{-1}. \end{aligned} \tag{51}$$

The main nonlinear term of Eq. (50) corresponds to the losses term; therefore we can expect that the maximum amplitude of oscillation can be computed using Eq. (47) for case 2:

$$A_\kappa = \frac{2}{3\kappa\omega_0^2}\sqrt{1-4\omega_1^4} = 0{\cdot}4947\lambda\sqrt{1-4\omega_1^4}. \tag{52}$$

We can now show that the amplitude A_κ is a good estimate of the numerical computation of the maximum amplitude of Eq. (18) when we use the value of the parameters given in Table 1 and the volume of the compression chamber is defined by Eq. (48). Figure 13 shows the value of A_κ as well as the amplitude computed numerically for values of λ from 0 to 0·5. Both graphs match satisfactorily, even for large values of λ where the asymptotic approximation is no longer strictly valid.

Finally, it is interesting to observe the shape of the set of curves in Fig. 12, which have been computed in our numerical experiments. Each curve represents the maximum amplitude of the oscillation for a fixed value of the perturbation parameter λ given in Eq. (48). It is interesting to notice that the maximum of these curves does not correspond to the same value of Ω/ω_0. The line in Fig. 12 which joins these maxima bends towards the right side of the figure. Using the asymptotic calculations, we can observe that the linear part of Eq. (50) is given by $\omega_0^2(\lambda) + 5{\cdot}978\lambda\cos(\sigma\omega_0 t)$, where $\omega_0^2(\lambda) = 8{\cdot}391 + 2{\cdot}918\lambda^2$. In this case the linear frequency of Eq. (50) is a function of λ. Using the expression of $\omega_0^2(\lambda)$, we can compute

$$\Omega/\omega_0(\lambda) = \frac{2\times\sqrt{8{\cdot}391}}{\sqrt{8{\cdot}391 + 2{\cdot}918\lambda^2}} \simeq 2 + 0{\cdot}347\lambda^2. \tag{53}$$

Now we plot $(\Omega/\omega_0(\lambda))$ in Fig. 14 as well as the value of the maximum amplitudes computed numerically. The graph of $(\Omega/\omega_0(\lambda))$ is slightly above the numerical points. Nevertheless the asymptotic never differs more than 0·4% from the numerical calculations.

7 Energy balance

An important step in the study of the parametric resonance in an OWC is to compute the amount of energy that we must supply to the system in order to sustain the attained oscillation amplitude. The source of energy in our model, which was described in a previous section, corresponds to the work done by the piston which maintains the mean level of the water surface in the compression chamber (see Fig. 3). The energy output of this model comes from the damping terms of the OWC.

Lorenceau obtained a rate of change of energy which is proportional to $\dot{x}^2|\dot{x}|$ (see Eq. (6)) with which we can compute the amount of energy loss by the system during one oscillation. On the other hand, we can also obtain the work done by the piston during one oscillation. Our goal is to compare these two energies and to show the way they depend on the parameter λ. It is important to obtain these relations because we have shown how the maximum amplitude depends on λ. In this way, we can estimate the cost, in terms of energy, of obtaining a prescribed amplitude of oscillation in terms of this parameter.

We compute first the input energy, that is, the work done by the piston during one cycle. The force that the piston exerts corresponds to the difference of pressure between the compression chamber, $P(t)$, and the atmospheric pressure P_{A}. The variations of $P(t)$ come from the oscillation of the water column and the displacement of the piston. Let P_0 and V_0 be the corresponding value of the pressure and the volume of the compression chamber in equilibrium (without oscillations); in that case the steady-state pressure is $P_0 = P_{\mathrm{A}} - \rho g H$. If we consider an adiabatic compression, the volume and pressure in the compression chamber are related to the steady-state values by

$$PV^{\gamma} = P_0 V_0^{\gamma}. \tag{54}$$

The volume V changes in time and it depends on the position of the water column, $x(t)$, and also the position of the piston (see Eq. (48)); hence this volume can be written as follows:

$$V(t) = V_0 + \mathcal{A}_{\mathrm{c}} x(t) + \lambda V_0 \sin(2\omega_0 t), \tag{55}$$

where $\mathcal{A}_{\mathrm{c}}$ is the area of the column and $x(t)$ is the solution of Eq. (50), that is, $x(t) = A_k \sin(\omega_0 t)$ (see Eq. (52)).

We can use Eqs. (54) and (55), also defining $\hat{A}_k \lambda = A_k \mathcal{A}_{\mathrm{c}}$, and obtain the pressure of the compression chamber:

$$P(t) = P_0 \left(\frac{V_0}{V_0 + \hat{A}_k \lambda \sin(\omega_0 t) + \lambda V_0 \sin(2\omega_0 t)} \right)^{\gamma}. \tag{56}$$

The work done by the piston is the integral of the force $\mathcal{A}_{\mathrm{p}} P(t)$ and the velocity of the piston $v_{\mathrm{p}}(t)$ in one cycle:

$$W_{\mathrm{p}} = \int_0^{2\pi/\omega_0} \mathcal{A}_{\mathrm{p}} P(t) v_{\mathrm{p}}(t) \mathrm{d}t, \tag{57}$$

where $\mathcal{A}_{\mathrm{p}}$ is the area of the piston. We can see that $\mathcal{A}_{\mathrm{p}} v_{\mathrm{p}}(t) = \frac{\mathrm{d}}{\mathrm{d}t} V_{\mathrm{p}}(t)$, where V_{p} is the volume of the piston $V_{\mathrm{p}}(t) = \lambda V_0 \sin(2\omega_0 t)$.

In order to obtain an estimate of the work done by the piston, for small values of the parameter λ, we compute its Taylor expansion around $\lambda = 0$ up to order four. The estimated value of W_{p} is then

$$W_{\mathrm{p}} \simeq \int_0^{2\pi/\omega_0} P_0 \left(1 + \frac{\gamma g(t)}{V_0} \lambda + \frac{\gamma(\gamma+1) g^2(t)}{2V_0^2} \lambda^2 + \frac{\gamma(-3+5\gamma-\gamma^2)}{V_0^3} \lambda^3 \right) 2\lambda V_0 \omega_0 \cos(2\omega_0 t) \mathrm{d}t, \tag{58}$$

where $g(t) = \hat{A}_{\kappa} \sin(\omega_0) + V_0 \sin(2\omega_0 t)$. The value of this integral represents the amount of energy that we must supply to the OWC in order to keep the attained maximum oscillation of the water column:

$$W_{\mathrm{p}} \simeq -\frac{\pi}{2} P_0 \frac{\hat{A}_{\kappa}^2 \gamma(\gamma+1)}{V_0} \lambda^3. \tag{59}$$

We now compute the output energy of our system. The losses of the system correspond to the energy of the OWC which is lost every cycle. From Eq. (6), the amount of energy lost during each oscillation is

$$W_{\mathrm{L}} = \int_0^{2\pi/\omega_0} \frac{\mathrm{d}\mathcal{E}}{\mathrm{d}t}\mathrm{d}t = \int_0^{2\pi/\omega_0} \mathcal{A}_{\mathrm{c}}\rho\dot{x}^2(t)|\dot{x}(t)|\mathrm{d}t. \tag{60}$$

Substituting $\dot{x}(t) = \frac{\mathrm{d}}{\mathrm{d}t}(\hat{A}_\kappa\lambda\sin(\omega_0 t))$, we obtain:

$$W_{\mathrm{L}} = \frac{8}{3}\hat{A}_\kappa^3\omega_0^2\lambda^3. \tag{61}$$

We have obtained the input and output energy of our system. These two energies W_{p} and W_{L} must coincide because there are no other energy sources or sinks in the system.

It is important to remark that the work done by the piston and the losses of the OWC are proportional to λ^3, while the attained amplitude of oscillation of the water column depends linearly on the parameter λ. Therefore, the cost of the parametric oscillation in terms of energy is proportional to λ^3.

8 Conclusions

It has been shown that parametric resonance may be a novel way to induce larger oscillations in an OWC system. In classical mechanics, energy is transferred more efficiently by parametric resonance than when an external excitation occurs. The exponential growth of the amplitude provides a very fast response for any initial perturbation and the maximum attainable amplitude is greater than in common resonance.

With the type of energy losses found in typical OWCs, in parametric resonance, once the system reaches the maximum amplitude, the oscillation does not modulate even if it is not exactly in tune. This is in contrast to normal resonance where modulation always occurs when out of tuning. The absence of modulation in parametric resonance is due to the existence of two attractor points in Eqs. (44) and (45), which means that the amplitudes of oscillation A and B evolve to one of these attractor points such that their amplitude is maintained. This property depends on two facts: the dominant nonlinear term of the equation of motion is the losses term $\dot{x}|\dot{x}|$ and the main excitation of the system is the parametric resonance. In addition to this, the amplitude of the oscillation in parametric resonance is less sensitive to variations in the resonant frequency.

We have shown two possible implementations of the parametric excitation of an OWC. Figure 3 represents a simple method to produce parametric resonance, although in this particular scheme, normal-resonance terms compete with the parametric excitation. Therefore, we expect that the attained amplitude of oscillation of the water column comes from the combination of parametric and forcing resonances. Figure 4 shows that the initial oscillations correspond to those driven by the forcing terms. After some time, the oscillation amplitude behaves like a pure parametric resonator; in particular, we can appreciate that there is no modulation in the oscillation amplitude.

The size of the maximum oscillation amplitude comes from the contribution of the different excitation terms. We can compute this amplitude as the sum of the single contribution of each resonance. Considering the case of Eq. (12) and its corresponding nondimentional form (13), this last equation contains a small parameter $|\beta_{\mathrm{p}}| \ll 1$. The expansion of this equation in powers of β_{p} is shown in Eqs. (14)–(17). The main excitation terms of the system correspond to the parametric resonance $(\gamma+1)W\beta_{\mathrm{p}}\cos(\frac{\Omega}{\hat{\omega}}t)x$ and also the forcing term $W\beta_{\mathrm{p}}\cos(\Omega t)$. An important fact is that the parameter β_{p} appears linearly in both terms. If we take into account only the parametric excitation, the dependence of β_{p} in the amplitude of oscillation is of order $\mathcal{O}(\beta_{\mathrm{p}})$. For the case of forcing resonance, the amplitude is of order $\mathcal{O}(\sqrt{\beta_{\mathrm{p}}})$ [14, pp. 1210]. We can conclude that the main contribution to the oscillation amplitude corresponds to the forcing resonance if $|\beta_{\mathrm{p}}| \ll 1$ while the parametric resonance dominates the amplitude when β_{p} is of order one. Therefore, we can expect that amplitude exhibits two different rates of growth with respect to β_{p} as shown in Fig. 15. The transition point is the value of β_{p} where we have the intersection of the two straight lines.

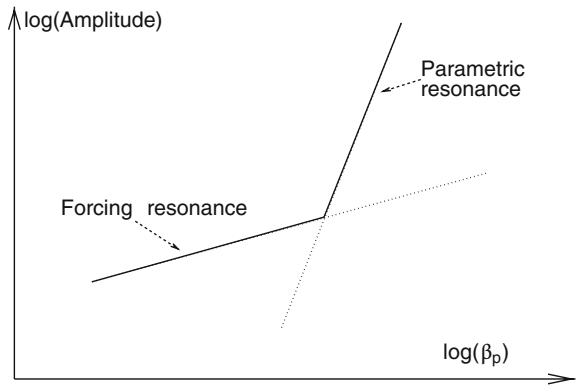

Fig. 15 Graph of the amplitude of oscillation versus the parameter β_p

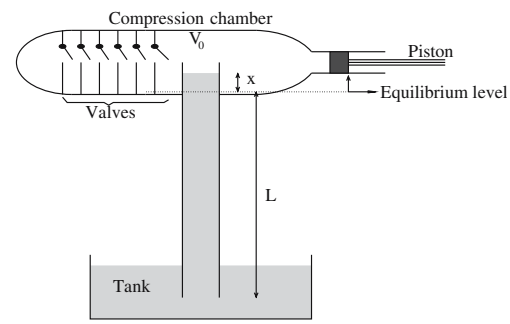

Fig. 16 Possible implementation of a parametric excitation of an OWC. The volume of the compression chamber is changed by the action of the piston and the aperture of the set of valves

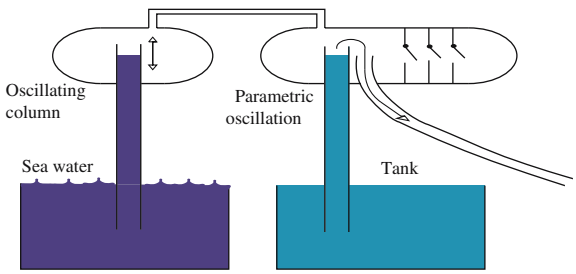

Fig. 17 Bi-directional water pump device

The implementation of a mechanical device which achieves only parametric resonance in an OWC is shown in Fig. 5. This device is more complex because we have added a mechanical valve in order to emulate the variation of the amount of air in the compression chamber. A better approach can be seen in Fig. 16 which shows an arrangement of valves to modify the amount of air in the compression chamber gradually. The piston attached to the main chamber modifies the equilibrium level of the water column. The behavior of these devices would be mainly driven by the parametric excitation.

Parametric resonance opens the way to new designs and different uses of OWCs. In the case of fluid pumps, not necessarily of seawater, this phenomenon could be used for bi-directional flow. Our proposal of the implementation of a bi-directional pump device which uses the energy of ocean waves is shown in Fig. 17. In this case the sea-water pump is excite by the volume variation of the compression chamber. The idea is to replace the oscillating piston in Fig. 16 with an oscillating water column which is in resonance with the ocean waves. This water column produces parametric resonance on the water pump. In this form, the water column supplies the power to the water pump, the energy being obtained from the water waves.

Acknowledgements The authors are grateful to Ana Cecilia Perez for the computer facilities in our laboratory. This work was supported by Grant CONACyT G25427-E and Proyecto Energía de Oleaje No. 139 del ICMyL-UNAM and Proyecto SEMARNAT–CONACYT CO1-0016.

References

1. Salter SH (1974) Wave power. Nature 249:720–724
2. McCormick M (1981) Ocean waves energy conversion. Wiley, New York

3. Malmo O, Reitan A (1985) Development of the Kvaerner Multiresonant OWC. In: Evans DV, Falcao AF (eds) Hydrodynamics of ocean wave-energy utilization. Springer-Verlag, Heidelberg, pp 57–67
4. Christensen L, Sorenses HC, Hansen LK (2005) Experience from the approval process of the Wave Dragon Proyect. In: Lewis A, Thomas G (eds) Fifth European Wave Energy Conference. Hydraulic & Maritime Research Center, Cork, Ireland, pp 332–338
5. Yemm RW, Henderson RM, Taylor CAE (2001) The OPD Pelamis WEC: Current status and onward programme. In: Ostergaad I, Iversen S (eds) Proceedings of Fourth European Wave Energy Conference. Energy Center Denmark. pp 104–109
6. Vriesema B (1995) The Archimedes wave swing: a new way of utilising wave energy. Report ECN-I–95-030. Energieonderzoek Centrum Nederland
7. Masuda Y (1986) An experience of wave power generator through tests and improvement. In: Evans DV, de Falco AF (eds) Proceedings of IUTAM Symposium an Hydrodynamics of Ocean Wave-Energy Utilization, Lisbon Portugal. Springer, Heidelberg, pp 445–452
8. Falnes J (2002) Ocean waves and oscillating systems. Cambridge University Press, Cambridge
9. Sarmento AJNA, de O Falcao AF (1985) Wave generation by an oscillating surface-pressure and its application in wave energy extraction. J Fluid Mech 150:467–485
10. Brito-Melo A, Hofmann T, Sarmento SJNA, Clément AH, Delhommeau G (1998) Hydrodynamic analysis of geometrical design parameters of oscillating water column device. In: Dursthoff WT (ed) Proceedings of Third European Wave Energy Conference. Patras, Greece. DruckTeam, Hannover, pp 23–30
11. McCormick M, Murtagh J, McCabe P (1998) Large-scale experimental study of a Hinged-Barge wave energy conversion system. In: Dursthoff WT (ed) Third European Wave Energy Conference. Patras, Greece. DruckTeam, Hannover, pp 215–222
12. Czitrom SPR, Godoy R, Prado E, Pérez P, Peralt-Fabi R (2000) Hydrodynamics of an oscillating water column sea-water pump: Part I theoretical aspects. Ocean Eng 27:1181–1198
13. Landau LD, Lifschitz EM (1978) Mechanics. Pergamon Press, New York
14. Czitrom SPR, Godoy R, Prado E, Olvera A, Stern C (2000) Hydrodynamics of an oscillating water column sea-water pump: Part II tuning to monochromatic waves. Ocean Eng 27:1199–1219
15. Lorenceau E, Quéré D, Ollitrault JY, Clanet C (2002) Gravitational oscillations of a liquid column. Phys Fluids 14:1185–1992
16. Knott GF, Flower JO (1980) Measurement of energy losses in oscillatory flow through a pipe exit. Appl Ocean Res 2:155–164
17. Cronin J (1980) Differential equations. Dekker, New York
18. McLachlan NW (1947) Theory and application of Mathieu functions. Oxford University Press, Oxford
19. Kevorkian J, Cole JD (1996) Multiple scale and singular perturbation methods. Applied mathematical sciences. Springer-Verlag, Heidelberg
20. Nayfeh AH (1973) Perturbation methods. John Wiley & Sons, Inc., New York
21. Tondl A, Ruijgrok T, Verhulst F, Nabergoj R (2000) Autoparametric resonances in mechanical systems. Cambridge Univ. Press, Cambridge
22. Guckenheimer J, Holmes P (1983) Nonlinear oscillation, dynamical system and bifurcation of vector fields. Springer-Verlag, Heidelberg